

The dimer to tetramer step appears to be required to stabilize the Mo(III,IV) unit which has the benefit of being held together by the EDTA ligand in a "basketlike" configuration. It is also of interest that Mo(III) and Mo(V) species are known to combine to give the Mo(IV) aquo trimer, but only at elevated temperatures (90 °C for ca. 1 h).¹⁹

Two stages were also observed in the O₂ oxidation of Mo(III)₂. Rate constants for the second stage (0.13–0.20 s⁻¹) overlap with the range of values obtained in the second stage with Co(C₂O₄)₃³⁻ as oxidant and could well correspond to the same process. Overall, however, a more complicated reaction sequence is likely with O₂, and unlike the O₂ oxidation of Mo³⁺¹¹ we are unable to comment further as to the detailed mechanism.

In conclusion, at least two stages are evident in the oxidation of Mo(III)₂ with both Co(C₂O₄)₃³⁻ and O₂. With Co(C₂O₄)₃³⁻ the first stage involving precursor ion-pair adduct formation followed by electron transfer is fairly well understood. Mechanistic assignments for the second observed stage are not as clearcut. Tentative suggestions include formation of a Mo(III,IV)₂ intermediate which decays in a first-order process giving a net disproportionation when Mo(III)₂ is in excess. This process is oxidant independent.

One general feature to note is the relative ease of oxidation of Mo(III)₂ as compared to Mo³⁺, with rate constants some 10² times faster for the dimer. This can be attributed to the ease of formation of the primary Mo(III,IV)₂ product as opposed to monomeric Mo(IV). The greater degree of hydrolysis of Mo(III) in the dimer may also favor reaction. It is unlikely

that reduction potentials for the monomer and dimer are identical.⁹

As far as substitution properties of Mo³⁺ and Mo(III)₂ are concerned, rate constants (25 °C) for the complexing of the aquo ions (2 × 10⁻³ M) with oxalate (2 × 10⁻² M) in 2.0 M HPTS can be compared. Values obtained are for Mo³⁺ (1.4 × 10⁻³ s⁻¹) and for Mo(III)₂ (1.6 × 10⁻⁴ s⁻¹). From this limited information, it appears that Mo(III)₂ is more inert than Mo³⁺. Kinetic studies on the 1:1 complexing of NCS⁻ and Cl⁻ with Mo³⁺ have been reported previously.²⁰

Bino²¹ has recently reported a study in which a new Mo(III) dimer, present in 1 M HCl as aquo Mo₂Cl₄²⁺, was identified. This ion (λ_{max} 430 nm) is believed to have an Mo–Mo triple bond and no bridging ligands. On addition of [Cl⁻] to the green aquo dimer in the present study, [Mo(III)₂] = 5 × 10⁻⁴ M, [HPTS] = 1.0 M, and [NaCl] = 1.0 M; no change in spectrum (Figure 1) was observed over 15 h at 25 °C. The separate existence of dimeric Mo(III) species with multiple Mo–Mo bonds on the one hand, and hydroxo bridging ligands on the other is interesting. No interconversion appears to take place for conditions so far examined.

Acknowledgment. We wish to acknowledge the award of a U.K. Science Research Council CASE Studentship (to M.A.H.) in collaboration with Molybdenum Climax Co.

Registry No. Mo(III), 51567-86-3; Co(C₂O₄)₃³⁻, 15053-34-6; IrCl₆²⁻, 16918-91-5; O₂, 7782-44-7; Mo₂O₄²⁺, 52757-71-8.

Supplementary Material Available: Table I listing rate constants (2 pages). Ordering information is given on any current masthead page.

(18) Shibahara, T.; Sykes, A. G. *J. Chem. Soc., Dalton Trans.* **1978**, 100.

(19) Souchay, P.; Cadiot, M.; Duhamaeux, M. *C. R. Hebd. Seances Acad. Sci., Ser. C* **1966**, 262, 1524.

(20) Sasaki, Y.; Sykes, A. G. *J. Chem. Soc., Dalton Trans.* **1975**, 1048.

(21) Bino, A. *Inorg. Chem.* **1981**, 20, 623.

Contribution No. 6408 from the Arthur Amos Noyes Laboratory, Division of Chemistry and Chemical Engineering, California Institute of Technology, Pasadena, California 91125

Electrochemical Generation of Monomeric Aquamolybdenum(V) by Reduction of Molybdenum(VI) at High Dilution in Trifluoromethanesulfonic Acid

MARK T. PAFFETT and FRED C. ANSON*

Received March 18, 1981

The electrochemistry of Mo(VI) in noncomplexing aqueous electrolytes is usually severely complicated by the oligomerization and subsequent adsorption of the reactant. This problem can be circumvented by employing dilute (≤10⁻⁴ M) solutions of Mo(VI) in 1–2 M trifluoromethanesulfonic acid. Under these conditions staircase voltammograms and pulse polarograms exhibit single, reversible waves that are consistent with the one-electron reduction of an unadsorbed, monomeric Mo(VI) species. The pH dependence of the reduction potentials suggests that two protons are consumed in the reduction of each Mo(VI). The monomeric Mo(V) reduction product undergoes spontaneous dimerization with a rate constant estimated as 10³ M⁻¹ s⁻¹. It also reduces perchlorate anions at a significant rate.

The electrochemical reduction of aquamolybdenum(VI) has been studied in a variety of supporting electrolytes.^{1–5} An early polarographic study¹ suggested the initial production of a chemically unstable Mo(IV) species while later work by Souchay and co-workers^{2,3} proposed that several forms (monomeric, tetrameric, etc.) of Mo(V) were produced and subsequently reduced to Mo(III). A report by Hull⁴ indicated that Mo(VI) is reduced in sulfuric acid to produce a Mo(V)

species that adsorbs on the electrode, but no structures of possible Mo(V) products were proposed. In all of the previous work the voltammetric responses were highly sensitive to the concentration of Mo(VI). Adsorption on the mercury electrodes was often invoked to account for complex voltammetric behavior although oligomerization of the variety of molybdenum(VI) oxo species present in homogeneous solutions has also been suggested.

The objective of the present work was to establish the nature of the initial product of the reduction of Mo(VI) at concentrations low enough to eliminate both adsorption and oligomerization in trifluoromethanesulfonic acid solutions.

Experimental Section

Materials. Trifluoromethanesulfonic acid (Minnesota Mining and Manufacturing Co.) was purified as previously described.⁶ The

(1) Haight, G. *J. Inorg. Nucl. Chem.* **1962**, 24, 673.

(2) Lamache, M.; Souchay, P. *J. Chim. Phys. Phys.-Chim. Biol.* **1973**, 2, 384.

(3) Lamache, M.; Cadiot, J.; Souchay, P. *J. Chim. Phys. Phys.-Chim. Biol.* **1968**, 65, 1921.

(4) Hull, M. J. *Electroanal. Chem. Interfacial Electrochem.* **1974**, 51, 57.

(5) Wittick, J.; Rechnitz, G. *Anal. Chem.* **1965**, 37, 816.

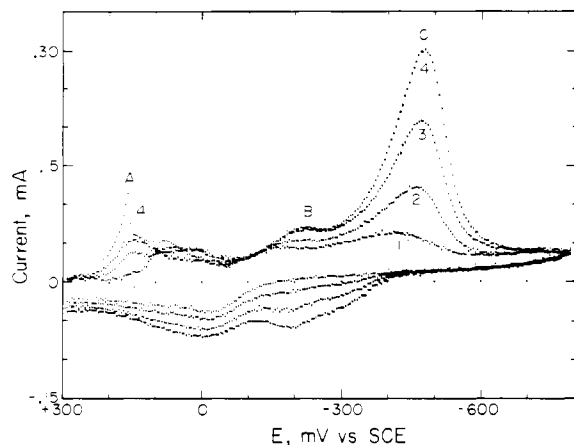


Figure 1. Cyclic staircase voltammograms of 0.5 mM Mo(VI) in 1.9 M $\text{CF}_3\text{SO}_3\text{H}$. Before the potential scan the mercury electrode was exposed to the solution for the intervals (1) 0.5, (2) 5.0, (3) 15.0, and (4) 45.0 s. The effective scan rate was 12.2 V s^{-1} .

purified acid was stored as the monohydrate in a refrigerator. Reagent grade sodium molybdate was used as received. *o*-Nitroaniline (Aldrich Chemical Co.) was recrystallized twice before use. Solutions were deoxygenated by bubbling with argon or nitrogen that had been passed successively through a solution of V(II) and over hot copper turnings. Solutions were prepared with triply distilled water or distilled water that was further purified by passage through a purification train (Barnstead Nanopure D2790). Solutions were checked for chloride impurities by pulse polarography. Impurity levels in 2 M solutions of trifluoromethanesulfonic acid were below $0.1 \mu\text{M}$. Stock solutions of Mo(VI) were standardized gravimetrically by precipitation of PbMoO_4 .

Instrumentation and Techniques. UV spectra were recorded on Cary 17, Varian 219, or Hewlett-Packard 8450 spectrophotometers. Electrochemical experiments were carried out in conventional compartmentalized cells. Experiments at variable temperatures were carried out in a cell with the working electrode compartment jacketed for temperature control. The reference electrode remained at room temperature. Most electrochemical measurements were performed with appropriate combinations of commercially available instruments (Princeton Applied Research Models 173, 174, 175, and 179). The Model 174 polarographic analyzer was modified to provide variable pulse width.⁷ Cyclic staircase voltammetry and chronocoulometry were carried out with a computer-based digital data acquisition and analysis system similar to that previously described.⁸ Staircase voltammetry⁹ was performed with a fixed step height of 4.88 mV. Variation of the effective sweep rate (i.e., (step height) \times (step width)⁻¹) was obtained by appropriate changes in the step widths. The area of the hanging mercury drop electrodes was 0.032 cm^2 . The dropping mercury electrode had a mercury flow rate of $1\text{--}1.5 \text{ mg s}^{-1}$. Potentials were measured and are quoted with respect to a saturated calomel reference electrode. The Hammett acidities of solutions of $\text{CF}_3\text{SO}_3\text{H}$ between 1 and 4 M were determined from the spectrum of *o*-nitroaniline indicator in each solution. Digital simulations of staircase voltammograms employed the method of Nicholson and Olmstead.¹⁰

Results

Voltammograms for the reduction of Mo(VI) in 1.9 M $\text{CF}_3\text{SO}_3\text{H}$ show several distinctive features that depend upon

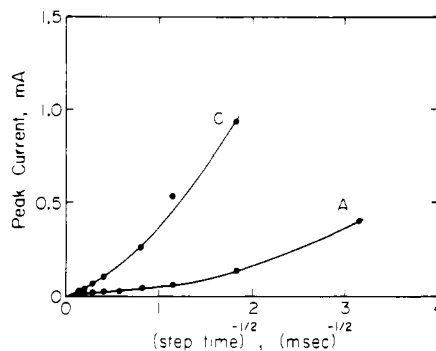


Figure 2. Dependence of peak current on $(\text{step time})^{-1/2}$, i.e., (effective scan rate)^{1/2}, for peaks A and C of Figure 1.

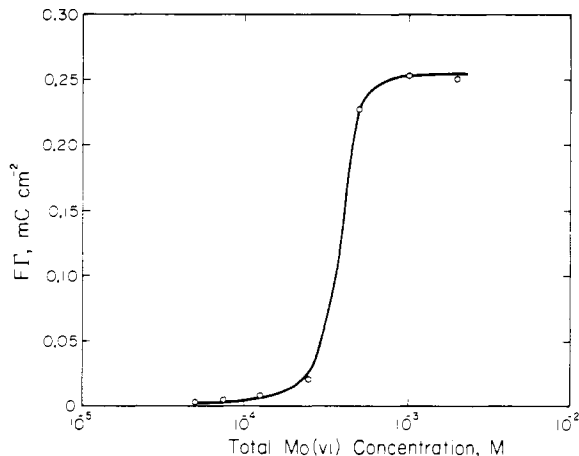


Figure 3. Adsorption of Mo(VI) at 0.3 V as a function of the concentration of Mo(VI). The potential was stepped from +0.3 to -0.6 V . The supporting electrolyte was 2 M $\text{CF}_3\text{SO}_3\text{H}$.

the concentration of Mo(VI) and the length of time that the mercury electrode is exposed to the solution. Figure 1 shows a set of cyclic staircase voltammograms for a 0.5 mM solution recorded after various times of exposure. Three reduction peaks are discernable (labeled A, B, and C in Figure 1); the most prominent peak appears near -0.5 V . Plots of peak currents vs. the square root of the effective scan rate (i.e., vs. $(\text{step time})^{-1/2}$) are shown for peaks A and C in Figure 2. (peak B is not well enough resolved at this concentration for a similar analysis.) The increasing positive deviations of the peak currents from the expected linear dependence on $(\text{step time})^{-1/2}$ is indicative of strong adsorption of the reactant, which also accounts for the otherwise unexpected dependence on electrode exposure time. At concentrations of Mo(VI) of 0.25 mM or less, peak B in Figure 1 is better resolved and exhibits a linear dependence of peak current on $(\text{step time})^{-1/2}$. Thus, peak B appears to correspond to the reduction of a diffusing reactant while peaks A and C are dominated by an adsorbed reactant.

At concentrations of Mo(VI) greater than ca. 0.5 mM the voltammetric responses become increasingly complex with obvious evidence of extensive adsorption. A variety of adsorbed species appears to be involved under these conditions, which we avoided in order to concentrate on the simpler behavior available with more dilute solutions.

Chronocoulometric Measurement of the Adsorption of Mo(VI). The extent of adsorption of Mo(VI) was estimated from the intercepts of single-step chronocoulometric charge-(time)^{1/2} plots.¹¹ The double-layer charging blank,

(6) Chalilpoyil, P.; Anson, F. *Inorg. Chem.* **1978**, *17*, 2418.
 (7) Abel, R.; Christie, J.; Jackson, L.; Osteryoung, J.; Osteryoung, R. *Chem. Instrum. (N.Y.)* **1976**, 123.
 (8) Lauer, G.; Abel, R.; Anson, F. *Anal. Chem.* **1967**, *39*, 765.
 (9) (a) Barker, G. C. *Adv. Polarography, Proc. Int. Congr., 2nd 1960*, *1*, 144. (b) Christie, J. H.; Lingane, P. J. *J. Electroanal. Chem.* **1965**, *10*, 176. (c) Mann, C. K. *Anal. Chem.* **1961**, *33*, 1484; (d) *Ibid.* **1965**, *37*, 326. (e) Zipper, J. J.; Perone, S. P. *Ibid.* **1973**, *45*, 452. (f) Ferrier, D. R.; Schroeder, R. R. *J. Electroanal. Chem. Interfacial Electrochem.* **1973**, *45*, 353. (g) Ryan, M. D. *Ibid.* **1977**, *79*, 105. (h) Miaw, H.-L.; Perone, S. P. *Anal. Chem.* **1978**, *50*, 1989.
 (10) Nicholson, R.; Olmstead, M. In "Electrochemistry: Calculations, Simulation and Instrumentation"; Marcel Dekker: New York, 1972; p 119.

(11) Bard, A. J.; Faulkner, L. R. "Electrochemical Methods"; Wiley: New York, 1980; p 199.

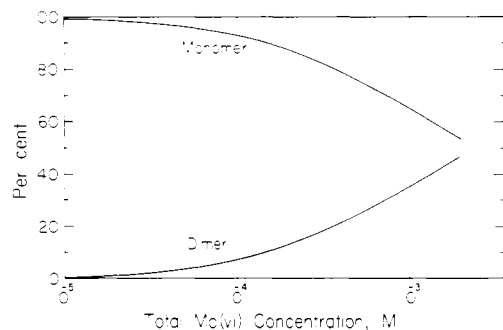


Figure 4. Distribution of Mo(VI) between monomeric and dimeric forms as a function of the concentration of Mo(VI) at 25 °C in 2 M $\text{CF}_3\text{SO}_3\text{H}$.

estimated from identical potential steps in the pure supporting electrolyte, was subtracted from each experimental intercept to obtain the quantity of adsorbed Mo(VI). Adsorption equilibrium was assumed to prevail when continued exposure of the electrode to the solution produced no further changes in the adsorption. Thirty seconds of exposure was usually sufficient for equilibrium to be reached. The results of these measurements are shown in Figure 3 for several initial electrode potentials. The most noteworthy feature for present purposes is the sharp decrease in adsorption at concentrations of Mo(VI) near 0.2–0.3 mM. Adsorption of Mo(VI) at concentrations below ca. 0.1 mM appears to be negligible.

Monomer–Dimer Equilibrium for Mo(VI). Equilibrium constants for the protonation and distribution of Mo(VI) among monomeric and dimeric forms in perchloric acid solutions have been evaluated from spectral measurements by Krumenacker and Bye^{12a} and by Cruywagen and co-workers.^{12b} We observed very similar spectra in solutions of Mo(VI) in $\text{CF}_3\text{SO}_3\text{H}$. We therefore utilized the procedure of ref 12a to estimate a conditional equilibrium constant for the monomer–dimer equilibrium in 2 M $\text{CF}_3\text{SO}_3\text{H}$:

$$K'_D = C_{\text{Mo}_2(\text{VI})} / (C_{\text{Mo}(\text{VI})})^2 \quad (1)$$

where $C_{\text{Mo}(\text{VI})}$ is the total concentration of monomeric Mo(VI) without regard to its state of protonation and $C_{\text{Mo}_2(\text{VI})}$ is the corresponding concentration of dimeric forms of Mo(VI). At 25 °C we found $K'_D = 4 \times 10^2 \text{ M}^{-1}$. (Cruywagen et al.^{12b} reported a value of $1.5 \times 10^2 \text{ M}^{-1}$ while Krumenacker and Bye^{12a} give a value of $3.4 \times 10^2 \text{ M}^{-1}$ in 1.5 M HClO_4 .)

Since we also found it desirable to examine the electrochemistry of Mo(VI) at 50 °C in 2 M $\text{CF}_3\text{SO}_3\text{H}$, we estimated a value for K'_D from spectral measurements at this temperature by assuming that the ratio of molar absorptivities reported by Cruywagen et al.^{12b} at 25 °C was maintained at 50 °C. We obtained $K'_D = 270 \text{ M}^{-1}$. A calculated distribution diagram for the sum of monomeric and dimeric forms of Mo(VI) at 25 °C is given in Figure 4. Note that there is no sharp change in the concentrations of the monomeric and dimeric species at bulk concentrations near 0.1–0.2 mM where the sharp increase in adsorption of Mo(VI) occurs (Figure 3). The implication is that the species responsible for the adsorption is not one of the predominant forms in solution but is produced on the electrode surface, possibly as a result of condensation reactions among the predominant solution species that are present at concentrations of Mo(VI) greater than ca. 0.2 mM but exhibit only weak adsorption.

Pulse Polarography. Normal and reverse pulse polarography^{13,14} were utilized to inspect the behavior of Mo(VI) at a

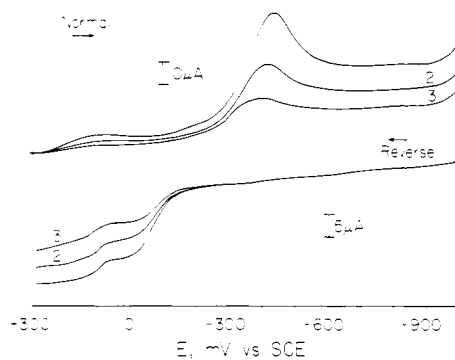


Figure 5. Normal and reverse pulse polarograms of 0.49 mM Mo(VI) in 2 M $\text{CF}_3\text{SO}_3\text{H}$. The drop time was 1 s. The pulse widths were (1) 10.5, (2) 18.2, and (3) 36.3 ms.

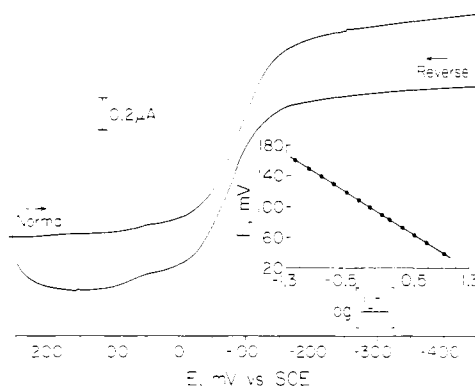


Figure 6. Normal and reverse pulse polarograms of 0.05 mM Mo(VI) in 2 M $\text{CF}_3\text{SO}_3\text{H}$. The drop time was 1 s and the pulse width 10.5 ms. The inset shows $-E$ vs. $\log [(i_L - i)/i]$ for the normal pulse polarogram.

dropping mercury electrode (Figure 5). At concentrations above 0.2 mM, normal pulse polarograms exhibited distorted shapes with current peaks preceding depressed limiting currents that signaled extensive adsorption of the reactant.¹⁵ Reverse pulse polarograms were free of such distortions. At concentrations below 0.1 mM normal pulse polarograms were also essentially undistorted (Figure 6). For a one-electron process the limiting reduction current in Figure 6, i_L , corresponds to a diffusion coefficient of $1.3 \times 10^{-5} \text{ cm}^2 \text{ s}^{-1}$ for Mo(VI) at this high dilution where it exists essentially entirely as a monomeric ion (Figure 4). The plot of E vs. $\log [(i_L - i)/i]$ shown in the inset in Figure 6 is linear with a slope of 57 mV pointing to a one-electron, Nernstian electrode reaction. Reverse pulse polarograms recorded from an initial potential of -0.45 V (where Mo(VI) is reduced to Mo(V) during the growth of each mercury drop before the potential is pulsed to more positive values) produced anodic limiting currents that were almost equal to the reduction currents obtained in the normal pulse polarograms of Mo(VI) so long as electrode drop times were restricted to 1 s or less. This is the behavior expected when a stable and reoxidizable reduction product is produced at the electrode surface.^{13,14} However, at longer drop times the ratio of anodic to cathodic currents decreased, as expected when the product of the electrode process, Mo(V) in the present case, is unstable.

A plot of the normal pulse polarographic half-wave potentials for the reduction of Mo(VI) as a function of Hammett acidity (recorded with drop times short enough to avoid significant decomposition of the reduction product) is shown in

(12) (a) Krumenacker, L.; Bye, J. *Bull. Soc. Chim. Fr.* **1968**, 3099. (b) Cruywagen, J. J.; Heyns, J. B. B.; Rohwer, E. F. C. H. *J. Inorg. Nucl. Chem.* **1978**, *40*, 53.

(13) Oldham, K.; Parry, E. *Anal. Chem.* **1970**, *42*, 229.

(14) Osteryoung, J.; Kirova-Eisner, E. *Anal. Chem.* **1980**, *52*, 62.

(15) Flanagan, J. B.; Takahashi, K.; Anson, F. C. J. *Electroanal. Chem. Interfacial Electrochem.* **1977**, *85*, 257.

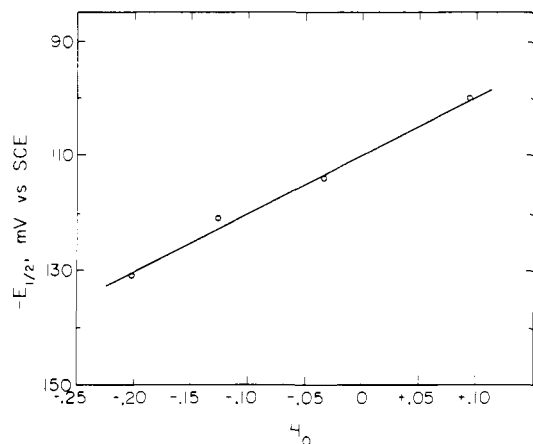


Figure 7. Polarographic half-wave potential vs. Hammett acidity function, H_0 , for reduction of monomeric Mo(VI) in $\text{CF}_3\text{SO}_3\text{H}$. The $\text{p}K_a$ of the *o*-nitroaniline indicator used to evaluate H_0 was taken as -0.3 .

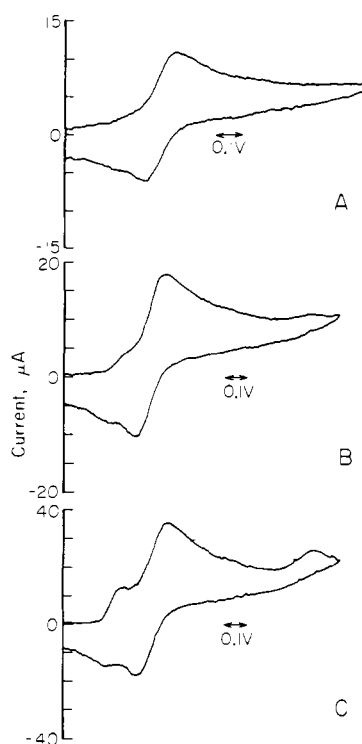


Figure 8. Cyclic staircase voltammograms for Mo(VI) in 2 M $\text{CF}_3\text{SO}_3\text{H}$ at 50 °C. The initial potential was +0.25 V and the step time 0.976 ms (effective scan rate = 5 V s^{-1}). Mo(VI) concentrations were (A) 0.098, (B) 0.24, and (C) 0.49 mM.

Figure 7. The slope of 102 mV is reasonably close to the 118-mV value expected if the one-electron reduction reaction consumed two protons.

Cyclic Staircase Voltammetry. Conventional cyclic voltammetry with reactant solutions as dilute as those required to eliminate the complications from oligomerization and adsorption of Mo(VI) yields current responses that are dominated by the capacitive background current. Cyclic staircase voltammetry eliminates much of this capacitive charging current⁹ and was therefore the preferred voltammetric method for these studies. Figure 8 shows a set of cyclic staircase voltammograms for several concentrations of Mo(VI). These voltammograms were recorded at 50 °C because at this temperature higher concentrations of Mo(VI) could be utilized without encountering the severe adsorption that occurs near room temperature. A reversible couple is clearly evident near -0.1

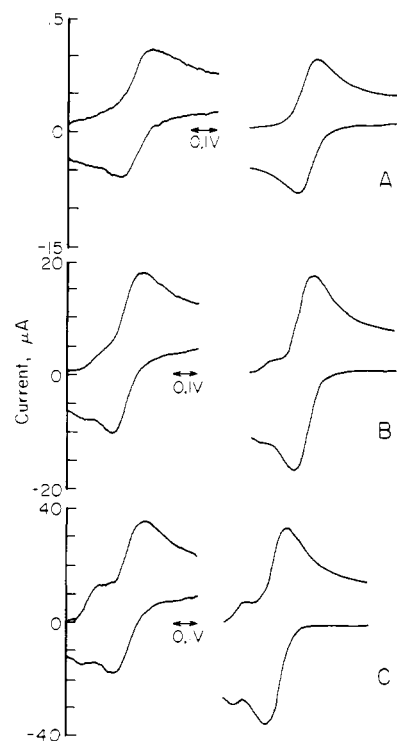


Figure 9. Comparison of experimental (left hand column) and simulated (right hand column) staircase voltammograms. The experimental voltammograms were taken from Figure 8 for potentials between +0.15 and -0.45 V .

V, and in contrast with the behavior at room temperature or in more concentrated solutions, there is no dependence of the peak currents or wave shapes on the length of time the electrode is exposed to the solution before the voltammogram is recorded. The cathodic and anodic peak currents are equal and linearly dependent on the square root of the effective scan rate between 2 and 100 V s^{-1} . However, at scan rates below ca. 2 V s^{-1} the anodic peak current falls below its cathodic counterpart as the decomposition of Mo(V) begins to deplete its concentration at the electrode surface.

The separation of peak potentials in the cyclic staircase voltammograms is dependent on the effective scan rate, and even at the lowest scan rates employed (1 V s^{-1}) it remained somewhat greater than the 80.6-mV value expected (at 50 °C) when a 4.88-mV staircase step height is applied to a Nernstian reaction.^{9b} It is probable that both uncompensated resistance and slow electron transfer contributed to this behavior, but we did not examine this feature in greater detail.

At concentrations of Mo(VI) greater than ca. 0.1 mM significant quantities of the dimeric ion are formed (Figure 4) and a wave which we believe to be due to the reduction of the dimer appears at more positive potentials in staircase voltammograms (Figure 8B,C). When the voltammograms were recorded at sufficiently high effective sweep rates ($>5 \text{ V s}^{-1}$), the monomer and dimer equilibrium was essentially "frozen" and the magnitudes of the two waves were compared with those calculated on the basis of the conditional equilibrium constant for the dimerization at 50 °C in 2 M $\text{CF}_3\text{SO}_3\text{H}$. Figure 9 shows a comparison of experimental staircase voltammograms with those obtained from a digital simulation of the staircase response for solutions containing a mixture of the monomeric and dimeric species. (The dimer was assumed to be reduced in a single, two-electron step and to have a diffusion coefficient 0.65 times as large as that of the monomer.) The reasonable agreement between the observed and simulated voltammograms supports the assignment of the first wave to the reduction of dimeric Mo(VI).

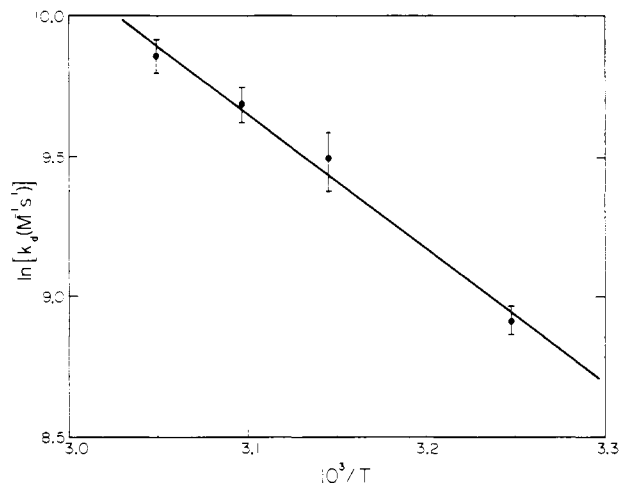


Figure 10. Arrhenius plot of chronocoulometrically determined rate constants governing the dimerization of Mo(V) monomer generated from 0.097 mM Mo(VI) in 2 M $\text{CF}_3\text{SO}_3\text{H}$.

The reduction of the familiar, dimeric form of molybdenum(V), $\text{Mo}_2(\text{V})$,¹⁶ is known to occur near -0.8 V.⁶ No wave corresponding to this process is evident in the staircase voltammograms for Mo(VI) when they are recorded at scan rates large enough to preserve equality of the anodic and cathodic peak currents. However, at lower scan rates, where smaller anodic to cathodic peak-current ratios result, a new wave begins to appear at the potential where $\text{Mo}_2(\text{V})$ is reduced to $\text{Mo}_2(\text{III})$ (Figure 8B,C).⁶ The clear implication is that the initial reduction product undergoes a subsequent reaction leading to the formation of the stable, reducible molybdenum(V) dimer, $\text{Mo}_2(\text{V})$.

Controlled-Potential Electrolysis. Reduction of a 0.1 mM solution of Mo(VI) at a stirred mercury pool at -0.25 V consumed 1 faraday/mol of Mo(VI). Voltammograms recorded during various stages of the electrolysis showed that a wave corresponding to the reduction of $\text{Mo}_2(\text{V})$ to $\text{Mo}_2(\text{III})$ developed as the original Mo(VI) reduction wave diminished. Thus, on the time scale of controlled-potential electrolyses (20–40 min) the reduction of monomeric Mo(VI) produces $\text{Mo}_2(\text{V})$.

Kinetics of the Disappearance of Mo(V). Chronocoulometry provides a convenient procedure for evaluating the rates of chemical reactions entered into by the products of an electrode reaction.¹⁷ The procedure involves the measurement of the ratio of faradaic charge consumed in the electrochemical production of an unstable species to the charge required for its subsequent electrochemical reconversion to starting material. This technique was applied to the Mo(VI)–Mo(V) system at a concentration of 0.1 mM and temperatures between 35 and 55 °C to minimize adsorption. The data were analyzed by means of a working curve derived from a published digital simulation of the case that the chemical reaction is a second-order dimerization reaction.¹⁸ (Attempts to fit the data to various first-order reaction schemes¹⁹ gave poorer fits to the corresponding working curves.) The resulting dimerization rate constant could be estimated only roughly because of complications from residual adsorption of Mo(VI) and the small signal-to-noise ratio. The values obtained at

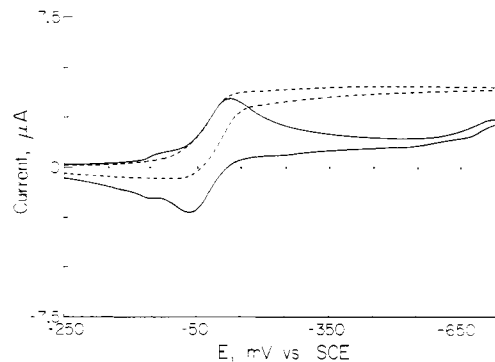


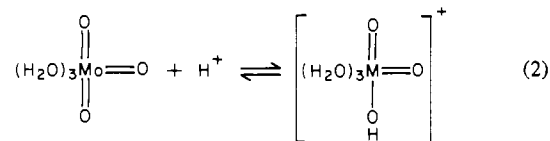
Figure 11. Effect of perchlorate on the cyclic staircase voltammograms of 0.097 mM Mo(VI). The supporting electrolytes were 2 M $\text{CF}_3\text{SO}_3\text{H}$ (—) and 1.9 M $\text{CF}_3\text{SO}_3\text{H}$ + 0.1 M HClO_4 (---); step time was 4.88 ms (effective scan rate 1 V s^{-1}).

several temperatures and their estimated precisions are shown in the Arrhenius plot in Figure 10. Extrapolation of the plot to 298 K leads to a rate constant of ca. 10^3 $\text{M}^{-1} \text{s}^{-1}$. The estimated activation enthalpy and entropy are 9 kcal/mol and -12 eu, respectively.

Catalyzed Reduction of Perchlorate. If moderate amounts of perchloric acid are added to dilute solutions of Mo(VI) in 2 M $\text{CF}_3\text{SO}_3\text{H}$, the resulting staircase voltammograms (Figure 11) exhibit the features expected for the catalyzed regeneration of a reactant from its reduction product.^{9b} Since $\text{Mo}_2(\text{V})$ does not react with perchlorate, the catalytically active species seems likely to be the monomeric form of Mo(V). At high scan rates the voltammogram is unaffected by perchlorate because the reaction between Mo(V) and perchlorate proceeds to an insignificant extent during the short period required to record the voltammogram. However, at lower scan rates, the cathodic current is enhanced, the wave shape becomes flat rather than peaked, and the anodic wave is diminished—all features consistent with the oxidation of Mo(V) by perchlorate.

Discussion

The important monomeric forms of Mo(VI) present in strongly acidic solutions were termed molybdic acid and protonated molybdic acid by Cruywagen et al.,^{12b} who wrote the formulas $\text{Mo}(\text{OH})_6$ and $\text{Mo}(\text{OH})_5\text{OH}_2^+$, respectively. We prefer to depict these two species as trioxo and *cis*-dioxo derivatives as in eq 2, for which Cruywagen et al.^{12b} report an

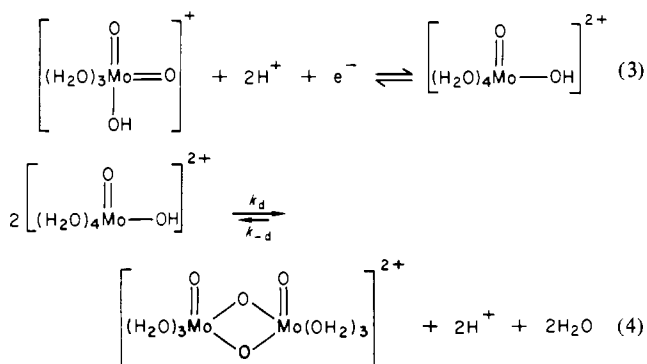


equilibrium constant of 11.4 M^{-1} (in 2 M HClO_4). Thus, in 2 M $\text{CF}_3\text{SO}_3\text{H}$ over 95% of the monomeric Mo(VI) would be present in the *cis*-dioxo form (with the assumption that the same equilibrium constant applies in $\text{CF}_3\text{SO}_3\text{H}$). As shown in Figure 4, dimer formation does not exceed a few percent with concentrations of Mo(VI) of 0.1 mM or less so that under these conditions the observed electrochemistry should be that of the *cis*-dioxo cation.

The pattern of electrochemical responses exhibited by dilute solutions of Mo(VI) is consistent with reactions 3 and 4 governing the course of the reduction. Reaction 3 takes account of the pH dependence of the half-wave potential for the reduction of Mo(VI) (Figure 7), and reaction 4 is based on a plausible structure that has been proposed for the stable dimer of Mo(V).^{16,20} Direct evidence for the reverse of reaction 4 is sparse: Murman has measured the kinetics of the

- (16) Cotton, F. A.; Wilkinson, G. "Advanced Inorganic Chemistry"; 4th ed.; Wiley: New York, 1980; p 868.
 (17) Christie, J. H. J. *Electroanal. Chem. Interfacial Electrochem.* 1967, 13, 79. Ridgeway, T. H.; Reilley, C. W.; Van Duyne, R. P. *Ibid.* 1976, 67, 1.
 (18) Childs, W.; Maloy, J.; Keszthelyi, C.; Bard, A. J. *J. Electrochem. Soc.* 1971, 118, 872.
 (19) Hanafey, M. K.; Scott, R. L.; Ridgeway, T. H.; Reilley, C. W. *Anal. Chem.* 1978, 50, 116.

- (20) Ardon, M.; Pernick, A. *J. Less-Common Met.* 1977, 54, 233.



exchange with the solvent of labeled bridging oxo groups in the Mo(V) dimer,²¹ but the mechanism of this process need not include the reverse of reaction 4. EPR signals for several monomeric complexes of Mo(V) have been reported,²² but such experiments have always involved the presence of added ligands that form very stable complexes with Mo(V).

The kinetics of dimerization of a monomeric Mo(V) catechol complex was reported recently²³ and a mechanism proposed that shares several of the features of reactions 3 and 4. However, large differences in pH and solution compositions prevent a more detailed comparison.

Since the Mo(V) monomer, but not the dimer,⁶ exhibits an anodic wave at -0.2 V (Figure 8), we sought to detect any monomer in equilibrium with the dimer by means of anodic normal pulse polarography with a 10 mM solution of Mo₂(V) prepared by exhaustive electrolytic reduction of Mo(VI) in 2 M CF₃SO₃H. No anodic response above background levels was detected in this experiment. We estimate that the maximum concentration of monomer that could have gone undetected as 6×10^{-6} M, which places a lower limit of ca. 10^9 M (25 °C) on the equilibrium constant for reaction 4 (assuming that the proton dependence is correct as shown).

The value estimated for the rate constant governing the dimerization of Mo(V), $k_d \sim 10^3 \text{ M}^{-1} \text{ s}^{-1}$ (25 °C), is qualitatively consistent with the behavior observed in the normal and reverse pulse polarographic experiments with 5×10^{-5} M solutions of Mo(VI) (Figure 5). For example, the ratio of anodic to cathodic limiting current decreased from unity to 0.71 as the drop time was increased from 1 to 5 s compared with a calculated value of 0.79 with the assumption of a simple, second-order irreversible loss of the Mo(V) throughout the 5-s drop life.

Although reoxidation of the monomeric form of Mo(V) to Mo(VI) appears to proceed readily at the mercury electrode, no further reduction of the monomer was observed before decomposition of the solvent commenced at ca. -1.0 V. This resistance of monomeric Mo(V) towards electroreduction to Mo(IV) matches the behavior of the monomeric Mo(III) ion, Mo(OH₂)₆³⁺, which is not oxidized to Mo(IV) at mercury electrodes.⁶ The apparent barrier to the generation of a monomeric form of aquamolybdenum(IV) is probably associated with the strong preference of this oxidation state to form multinuclear ions: The stable form of aquamolybdenum(IV)

has been argued to contain one,²⁴ two,²⁵ and three^{21,26} molybdenum centers, but there is a growing consensus favoring the trimeric ion, Mo₃O₄⁴⁺, as the likely species present in aqueous acid.^{21,26} The differences in the structures of monomeric Mo(III) ion, Mo(OH₂)₆³⁺, and that proposed for monomeric Mo(V) in eq 3 do not appear to be large, but the difficulty in passing through the evidently unstable monomeric Mo(IV) state to reach Mo(OH₂)₆³⁺ is presumably responsible for the absence of a two-electron reduction of the Mo(V) monomer. In an earlier report⁶ on the pulse polarography of monomeric Mo(OH₂)₆³⁺ (with the initial electrode potential at +0.15 V) a prominent reduction wave was observed near -0.1 V that was tentatively ascribed to the reduction of monomeric Mo(V) generated at the electrode surface by oxidation of Mo(OH₂)₆³⁺. The present results indicate that monomeric Mo(V) is not reducible in the accessible potential range but that the reduction of monomeric Mo(VI) proceeds near -0.1 V. For these reasons we are now inclined to assign the wave at -0.1 V in the pulse polarography of Mo(OH₂)₆³⁺ to the reduction of Mo(VI) monomer generated by the (very slow)⁶ oxidation of Mo(OH₂)₆³⁺ at +0.15 V.

The sudden onset of extensive adsorption of Mo(VI) at bulk concentrations greater than ca. 0.2 mM (Figure 3) is not typical of simple ionic adsorption at mercury.²⁷ It is more reminiscent of adsorption that appears to result in the formation of new phases containing multilayers of the adsorbate on the surface.²⁸ The behavior of Mo(VI) differs from most previous examples²⁹ in that no complex-forming ligands are required to induce the adsorption. The well-known tendency for Mo(VI) to condense spontaneously into oligomeric ions as its concentration is increased³⁰ seems likely to underlie the adsorption. At concentrations above 1 mM or so the electrode surface appears to become covered with a film of condensed polymolybdate of unknown composition that interferes with the reduction of Mo(VI) from the bulk of the solution, leading to the distorted and depressed polarograms and voltammograms that are so familiar in the electrochemistry of Mo(VI).¹⁻⁵

Conclusions

Highly dilute acidic solutions of Mo(VI) in which monomeric ions predominate exhibit much simpler electrochemistry than results with less dilute solutions. A reversible redox couple consisting of monomeric Mo(VI) and Mo(V) ions can be observed in such solutions. The aquamolybdenum(V) ion undergoes spontaneous dimerization to form the stable Mo₂(V) ion, which is not oxidizable at mercury electrodes. The monomeric form of Mo(V) is not further reduced in the accessible range of potentials probably because of the intrinsic instability of the monomeric Mo(IV) that would result. Monomeric Mo(V) is catalytically active toward reduction of perchlorate.

Acknowledgment. This work was supported by the National Science Foundation.

Registry No. MoO₂(OH)(OH₂)₃⁺, 78939-74-9; MoO(OH)(OH₂)₄²⁺, 78939-75-0.

- (21) Murman, K. *Inorg. Chem.* **1980**, *19*, 1765.
 (22) Sacconi, L.; Cini, R. *J. Am. Chem. Soc.* **1954**, *76*, 4239. Spence, J. T.; Heydaneck, M. *Inorg. Chem.* **1967**, *6*, 1489. Huang, T. J.; Haight, G. P., Jr. *J. Am. Chem. Soc.* **1970**, *92*, 2336; **1971**, *93*, 611. Imamura, T.; Haight, G. P., Jr.; Belford, R. L. *Inorg. Chem.* **1976**, *15*, 1047. Haight, G. P.; Woltermann, G.; Imamura, T.; Hummel, P. *J. Less-Common Met.* **1977**, *54*, 121.
 (23) Charney, L. M.; Schultz, F. A. *Inorg. Chem.* **1980**, *19*, 1527.

- (24) Ojo, J. F.; Sasaki, Y.; Taylor, R.; Sykes, A. G. *Inorg. Chem.* **1976**, *15*, 1006.
 (25) Ardon, M.; Bino, A.; Yahav, G. *J. Am. Chem. Soc.* **1976**, *98*, 2338. Cramer, S. P.; Gray, H. G.; Dori, Z.; Bino, A. *Ibid.* **1979**, *101*, 2770.
 (26) (a) Richens, D. T.; Sykes, A. G. *Comments Inorg. Chem.* **1981**, *1*, 141. (b) Cramer, S. P.; Slusser, P.; Gray, H. B. *J. Am. Chem. Soc.*, in press.
 (27) Delahay, P. "Double Layer and Electrode Kinetics"; Wiley-Interscience: New York, 1965; Chapter 4.
 (28) Elliott, C. M.; Murray, R. W. *J. Am. Chem. Soc.* **1974**, *96*, 3321. Parkinson, B. A.; Anson, F. C. *Anal. Chem.* **1978**, *50*, 1886.
 (29) Anson, F. C. *Acc. Chem. Res.* **1975**, *8*, 400.
 (30) Reference 16, p 852 ff.